Supporting Information

Gram-Scale Synthesis of Carbon Quantum Dots with Large Stokes Shift Enables Fabrication of Eco-Friendly and High-Efficiency Luminescent Solar Concentrators

Haiguang Zhao,*[a,b] Guiju Liu,[b] Shujie You,[c] Franco V. A. Camargo,[d] Margherita Zavelani-Rossi,[d] Xiaohan Wang,[a,e] Changchun Sun,[a,e] Bing Liu,[a] Yuanming Zhang,[a] Guangting Han,[a] Alberto Vomiero*[c,f] and Xiao Gong*[,g]

[a.] *State Key Laboratory of Bio-Fibers and Eco-Textiles, Qingdao University, No. 308 Ningxia Road, Qingdao 266071, P.R. China Email: hgzhao@qdu.edu.cn*

[b.] *College of Physics, University Industry Joint Center for Ocean Observation and Broadband Communication, Qingdao University, No. 308 Ningxia Road, Qingdao 266071, P.R. China*

[c.] *Division of Materials Science, Department of Engineering Sciences and Mathematics, Luleå University of Technology, 971 87 Luleå, Sweden*

[d.] *Dipartimento di Fisica & Dipartimento di Energia, Politecnico di Milano, via G. Ponzio 34/3 and IFN-CNR, piazza L. da Vinci 32, 20133 Milano, Italy*

[e.] *College of Textiles & Clothing, Qingdao University, No. 308 Ningxia Road, Qingdao 266071, P.R. China*

[f.] *Department of Molecular Science and Nano Systems, Ca' Foscari University of Venice Via Torino 155, 30172 Venezia Mestre, Italy alberto.vomiero@ltu.se*

[g.] *State Key Laboratory of Silicate Materials for Architectures, Wuhan University of Technology, 122 Luoshi Road, Wuhan 430070, Hubei, P.R. China xgong@whut.edu.cn*

Supporting Figures and Tables:

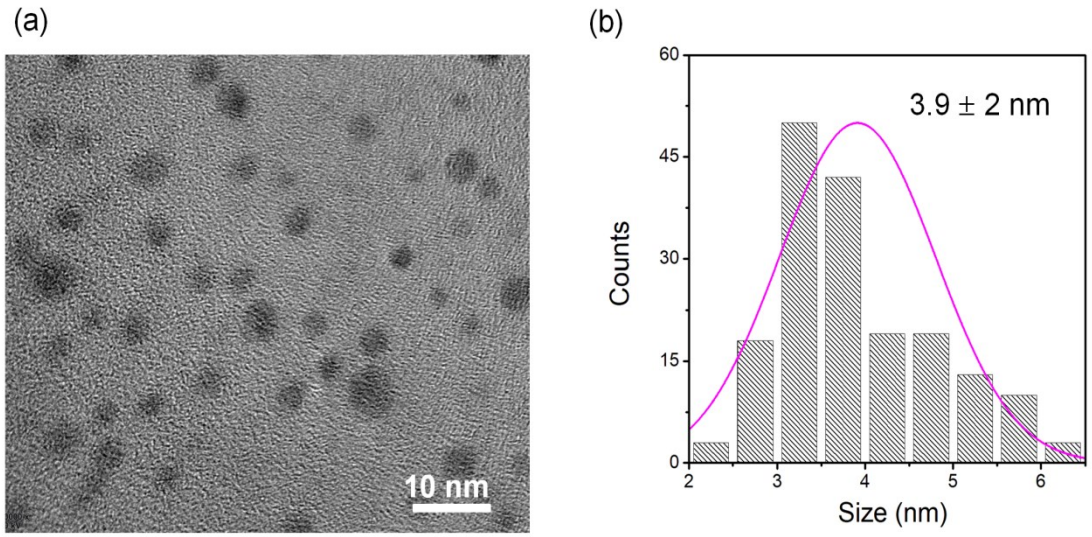

Fig. S1 (a) Representative TEM images of C-dots synthesized via solvothermal reaction. (b) Size distribution of C-dots.

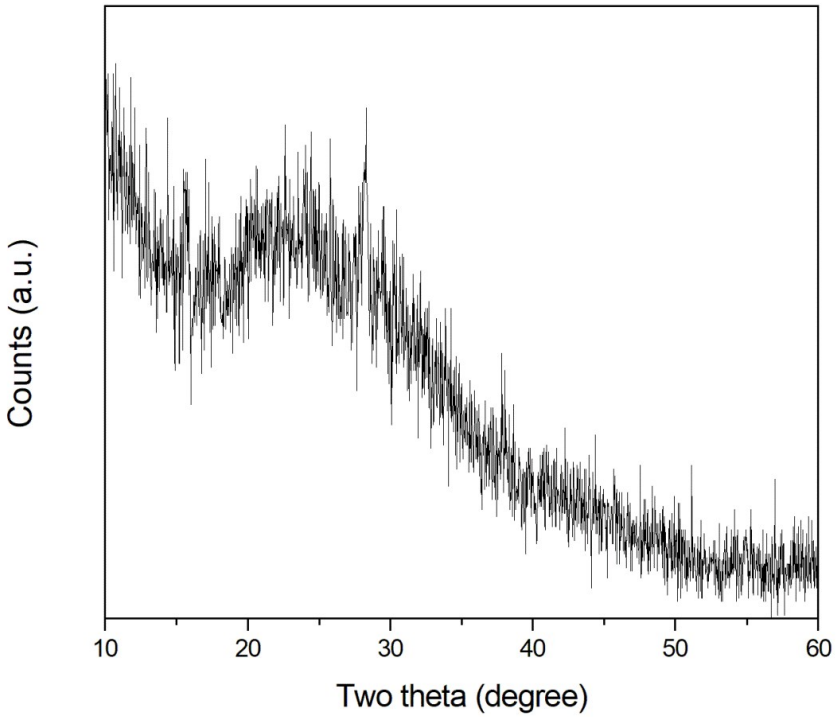

Fig. S2 XRD pattern of the C-dots synthesized via space-confined vacuum heating approach.

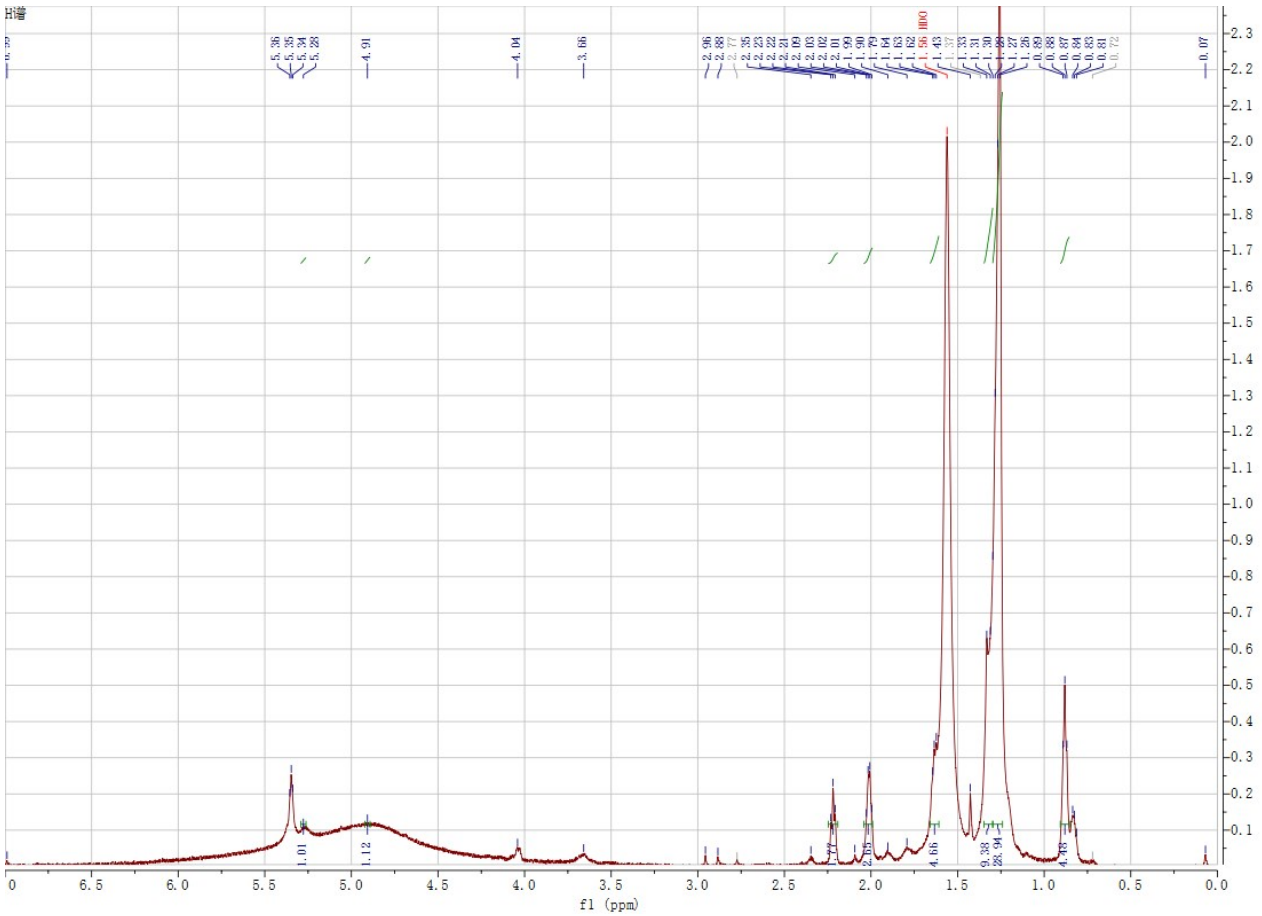

Fig. S3 ^{1}H NMR spectra of C-dots synthesised via vacuum heating approach. The C-dots were prepared via a vacuum heating approach. After purification, the C-dots were dried under vacuum for 12 hour. The powder C-dots were redispersed in deuterated methanol for NMR measurement.

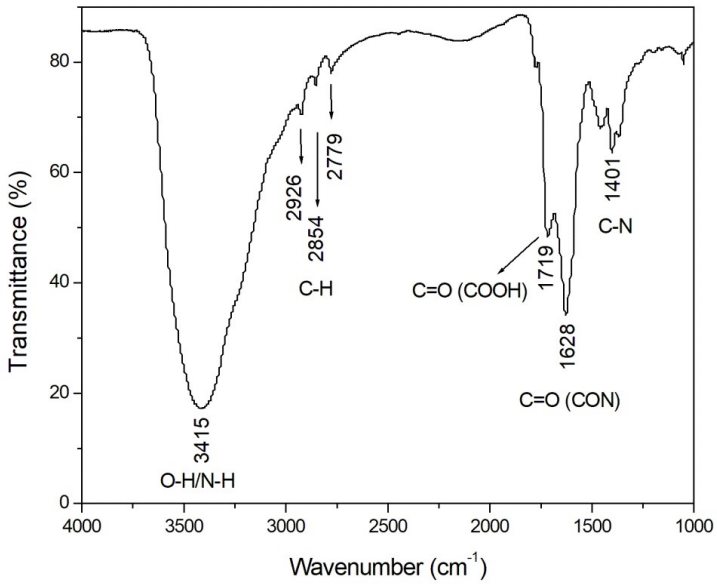

Fig. S4 FI-IR spectrum of the as-purified C-dots synthesised via vacuum heating approach. The C-dots were prepared via a vacuum heating approach. After purification, the C-dots were dried under vacuum for 12 hour. The powder C-dots were directly measured by FT-IR in in reflection mode.

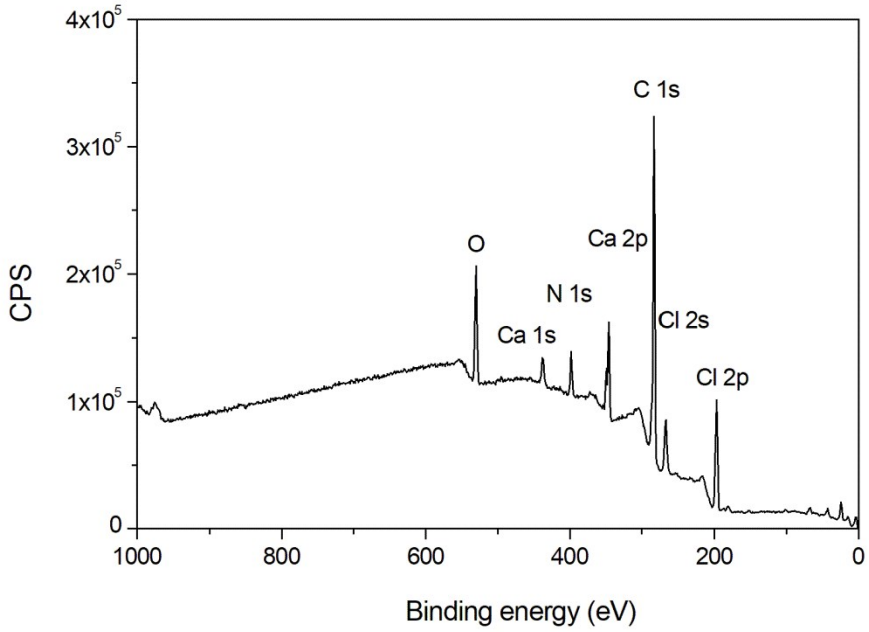

Fig. S5 XPS spectra of the C-dots. The C-dots were prepared via a vacuum heating approach. After purification, the C-dots methanol solution was dropped on FTO glass for XPS measurement.

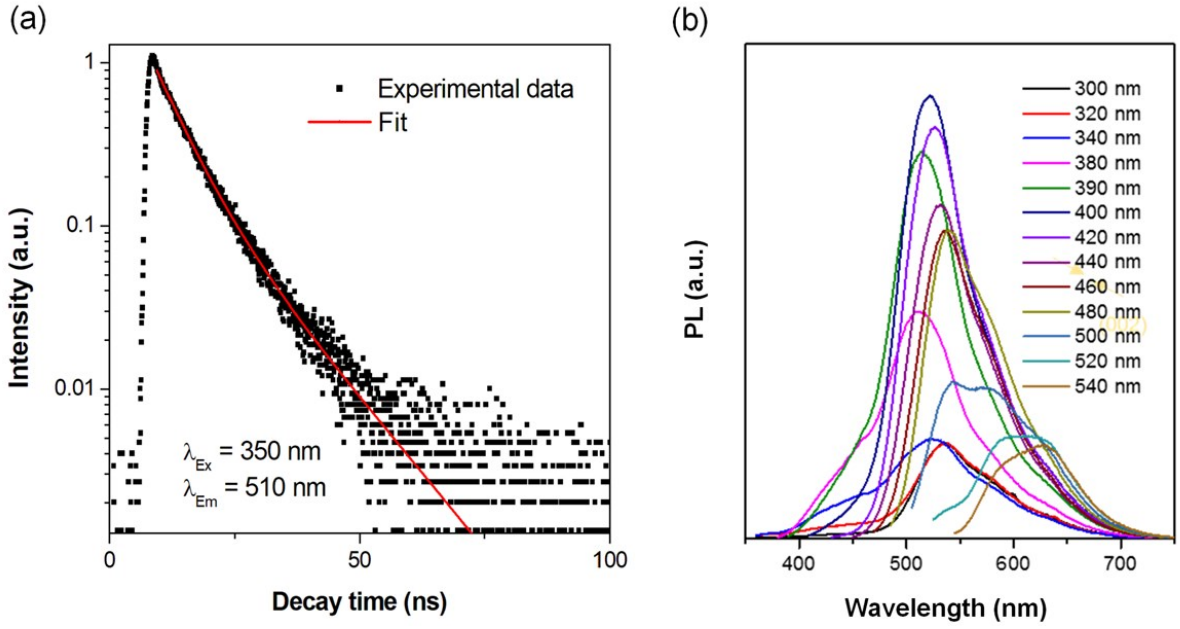

Fig. S6 The PL decay from C-dots with pulsed LED at 350 nm. (b) PL spectra of C-dots in methanol. The C-dots were synthesized via the solvothermal method using citric acid and urea as precursors.

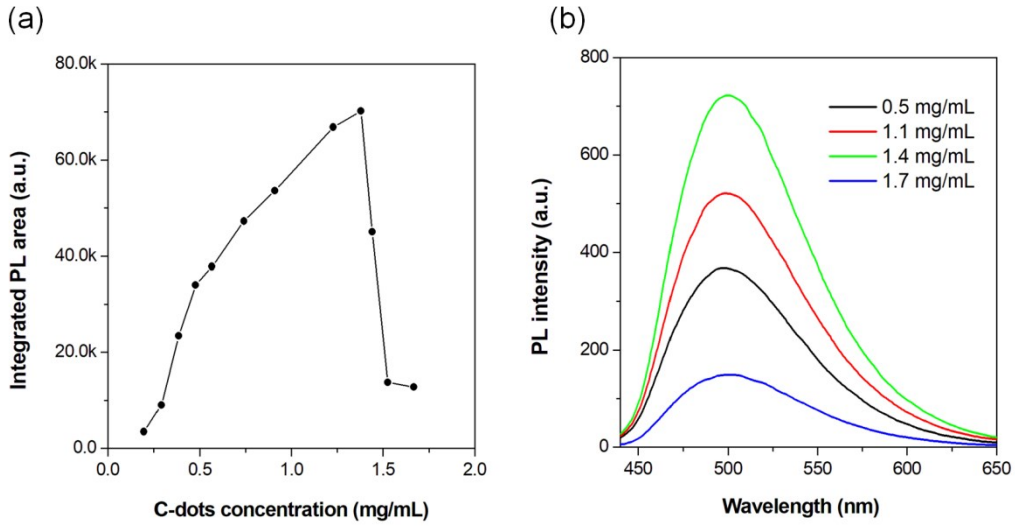

Fig. S7 Integrated PL area (a) and PL spectra (b) of the C-dots in methanol as a function of C-dots concentration. The C-dots were produced via vacuum heating approach.

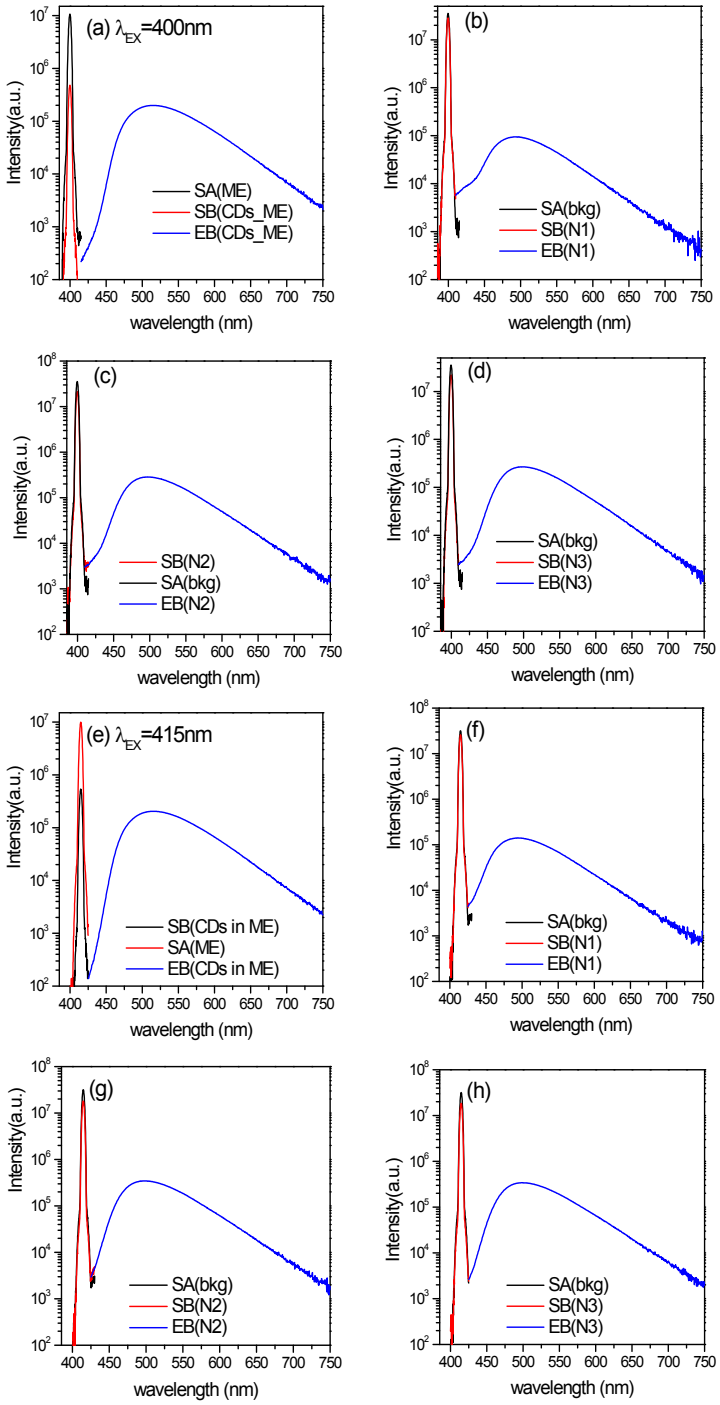

Fig. S8 The PL spectra collected in integration sphere. The excitation wavelength is 317 nm. In each figure the red, black and blue curves refer to the scattering from a blank reference (SA) and the sample (SB), and the emission from the sample (EB), respectively. SA(ME) refers the scattering from methanol and SA(bkg) refers to the scattering from the empty integrating sphere. N1, N2 and N3 are glass samples coated with C-dots/pvp film; the thickness of the coated C-dots/pvp film increases from N1 to N3.

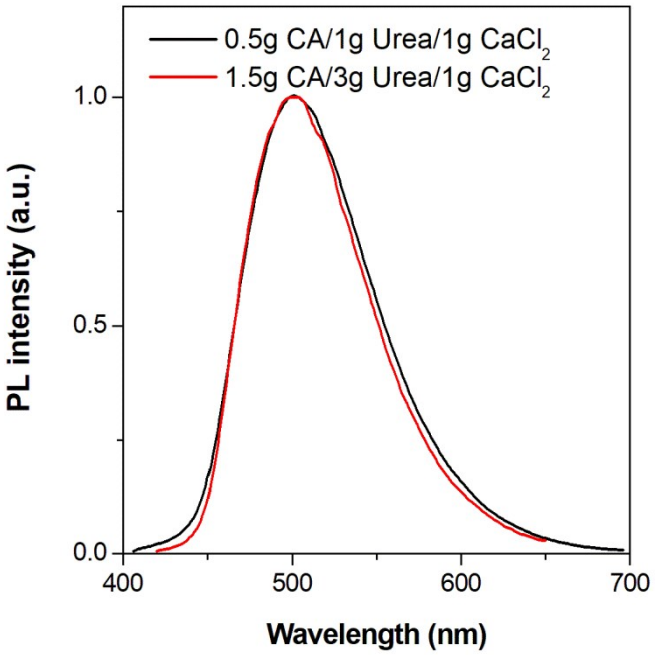

Fig. S9 PL spectra of the C-dots synthesized via a vacuum heating method using different recipe. The C-dots were dispersed in methanol for PL measurement.

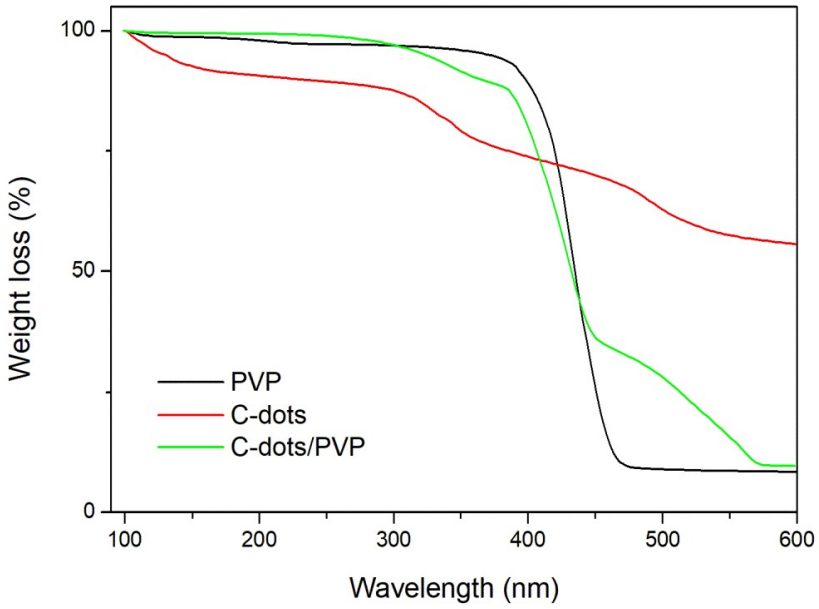

Fig. S10 Thermogravimetric analysis (TGA) curves of C-dots, PVP (equal mass of K30/K90) and C-dots/PVP hybrid. The TGA was carried out in air at 10 ^{o}C/min. Weight loss at different temperatures indicates the decomposition as well as thermal stability of the samples. The total weight loss of PVP reaches 90.2% from 100 ^{o}C to 600 ^{o}C. The pure C-dots show multiple losses in weight. The total weight loss of C-dots reaches 44% from 100 ^{o}C to 600 ^{o}C. Based on TGA data, the C-dots concentration is 2 wt% in C-dots/PVP film.

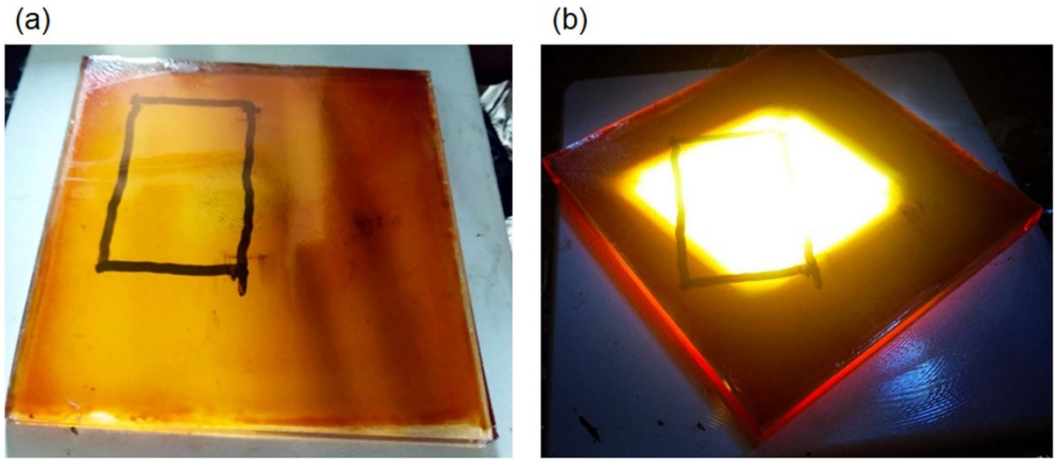

Fig. S11 Photographs of the LSC under indoor (uncharacterized spectrum) (a), and simulated sunlight (calibrated solar simulator, AM1.5G, 100 mW/cm^2) (b) fabricated by using solvothermal C-dots. We clearly see the rectangle in Fig. S12a, indicating the semitransparency of the LSC using the solvothermal C-dots. A clear red color on the edges of the LSC indicates the strong reabsorption due to the overlap between the emission and absorption spectra, which leads to energy loss in the short-wavelength, as expected from the low Stokes shift.

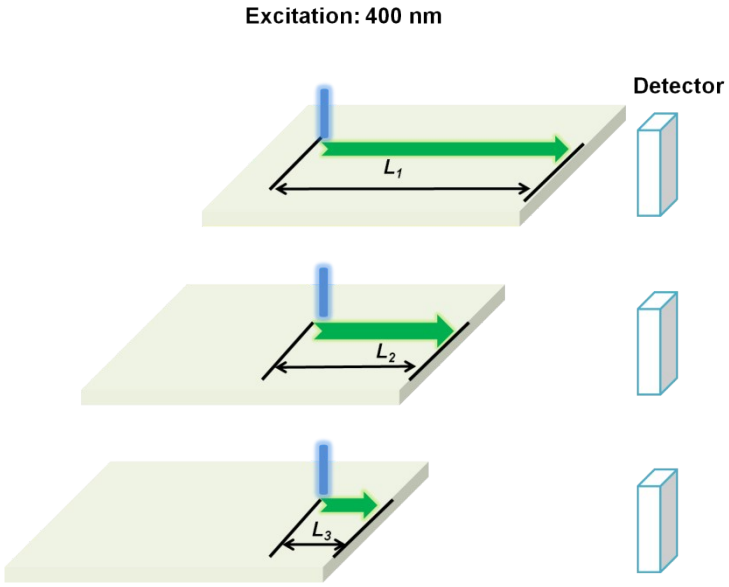

Fig. S12 PL set up for measuring the distance dependent optical behaviour in the LSC based on C-dots. During the measurement, only the LSC was moved with the fixed position of excitation beam and detector. The excitation beam (wavelength and power density) is identical for all measurements.

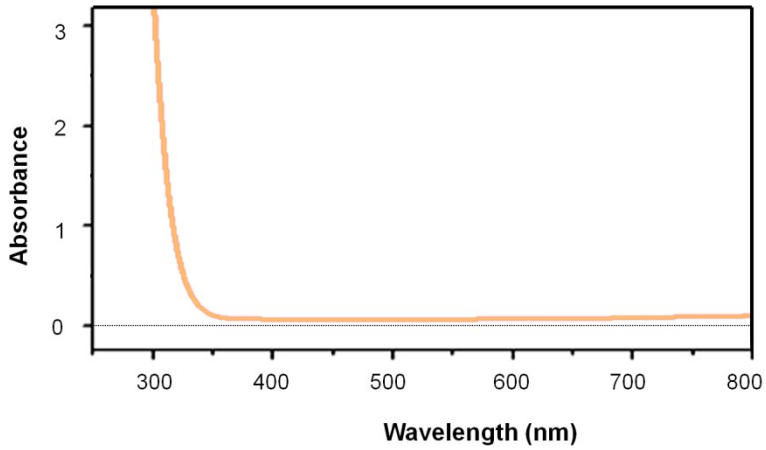

Fig. S13 Absorbance of the PVP/glass substrate. The PVP film was prepared by drop-casting approach. The PVP concentration is 200 mg/mL and the quantity of the PVP K30 and K90 is identical.

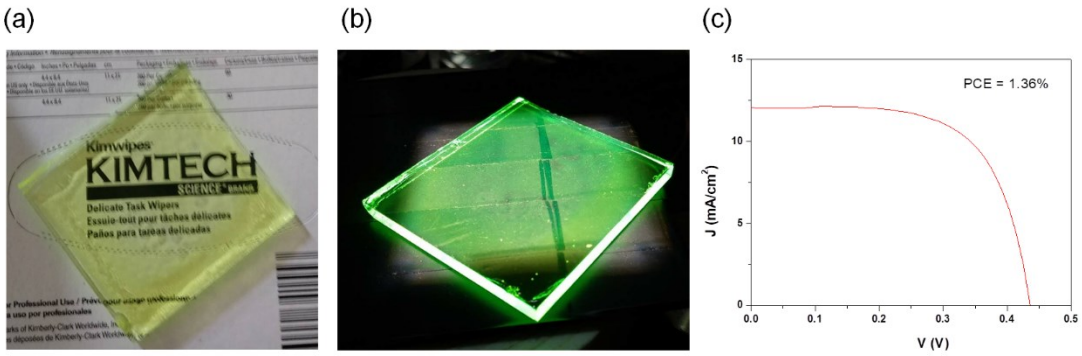

Fig. S14 Small area (5×5 cm^2) LSC under (a) internal ambient light and (b) solar simulator (standard AM1.5G, 100 mW/cm^2). (c) Current density versus voltage curve of a Si solar cell used to calculate the PCE of the (5×5 cm^2) LSC under AM1.5G (100 mW/cm^2) calibrated irradiation.

Table S1 Biexponential fitting of lifetime data, λ_{Ex}=372nm.

	τ_1 (ns)	τ_2 (ns)	B_1	B_2	τ_{av} (ns)
C-dots in methanol[a] (vacuum heating)	12.2(3)	15.6(8)	77(12)	23(13)	13.1
C-dots in LSCs[a]	8.3(3)	14.7(1)	22(2)	78(2)	13.8
C-dots in methanol[b] (solvothermal)	1	7.4	30	70	7

[a] C-dots were synthesized via vacuum heating approach;

[b] C-dots were synthesized via solvothermal reaction.

Biexponential fitting was employed to fit the lifetime data.

The average lifetime was calculate through equation $\tau_{PL} = \frac{B_1\tau_1^2 + B_2\tau_2^2}{B_1\tau_1 + B_2\tau_2}$

Table S2. Optical properties of LSCs fabricated using carbon dots synthesized *via* a hydrothermal approach or vacuum heating approach.

	C-dots (solvothermal)	**C-dots (vacuum heating)**	
LSC dimension	10×10×0.5 cm^3	10×10×0.5 cm^3	5×5×0.5 cm^3
First excitonic absorption peak position	455 nm	400 nm	
PL peak position	524 nm	500 nm	
Stokes shift	360 meV	530 meV	
External optical efficiency of LSCs (natural light, uncharacterized spectrum, 100 mW/cm^2)	0.7±0.1%	2.2±0.1%	/
External optical efficiency of LSCs (solar simulator, AM1.5G, 100 mW/cm^2)	/	/	3.0%
Retaining integrated PL intensity after 2 h UV illumination (400 nm, 500 mW/cm^2) for LSCs	80%	77%	/
External optical efficiency of LSCs stored under the dark for 6-months (20 °C with humidity of 40%)	0.7±0.1%	2.2±0.1%	/

References

1. Li, H., Wu, K., Lim, J., Song, H.-J. & Klimov, V.I. Doctor-blade deposition of quantum dots onto standard window glass for low-loss large-area luminescent solar concentrators. Nat. Energy 1, 16157 (2016).

2. Wu, K.F., Li H.B., and Klimov, V.I. Tandem luminescent solar concentrators based on engineered quantum dots, Nature Photonics, 2018, 12, 105-110.

3. Lewis, N.S. Research opportunities to advance solar energy utilization. Science 351, 10.1126/science.aad1920 (2016)